

POLSKA AKADEMIA NAUK

INSTYTUT MASZYN PRZEPEŁYWOWYCH

**TRANSACTIONS  
OF THE INSTITUTE OF  
FLUID-FLOW MACHINERY**

PRACE

INSTYTUTU MASZYN PRZEPEŁYWOWYCH

103



GDAŃSK 1997

THE TRANSACTIONS OF THE INSTITUTE OF FLUID-FLOW MACHINERY

---

exist for the publication of theoretical and experimental investigations of all aspects of the mechanics and thermodynamics of fluid-flow with special reference to fluid-flow machines

\*

PRACE INSTYTUTU MASZYN PRZEPIYWOWYCH

---

poświęcone są publikacjom naukowym z zakresu teorii i badań doświadczalnych w dziedzinie mechaniki i termodynamiki przepływów, ze szczególnym uwzględnieniem problematyki maszyn przepływowych

*Wydanie publikacji dofinansowane zostało przez PAN ze środków DOT uzyskanych z Komitetu Badań Naukowych*


EDITORIAL BOARD – RADA REDAKCYJNA

ZBIGNIEW BILICKI \* TADEUSZ GERLACH \* HENRYK JARZYNA  
JAN KICIŃSKI \* JERZY KRZYŻANOWSKI (CHAIRMAN – PRZEWODNICZĄCY)  
WOJCIECH PIETRASZKIEWICZ \* WŁODZIMIERZ J. PROSNAK  
JÓZEF ŚMIGIELSKI \* ZENON ZAKRZEWSKI

EDITORIAL COMMITTEE – KOMITET REDAKCYJNY

EUSTACHY S. BURKA (EDITOR-IN-CHIEF – REDAKTOR NACZELNY)  
JAROSŁAW MIKIELEWICZ  
EDWARD ŚLIWICKI (EXECUTIVE EDITOR – REDAKTOR) \* ANDRZEJ ŻABICKI

EDITORIAL OFFICE – REDAKCJA

Wydawnictwo Instytutu Maszyn Przepływowych  
Polskiej Akademii Nauk  
ul. Gen. Józefa Fiszera 14, 80-952 Gdańsk, skr. poczt. 621,  
 (0-58) 46-08-81 wew. 141, fax: (0-58) 41-61-44,  
e-mail: esli@imppan.imp.pg.gda.pl

ISSN 0079-3205

MARIAN TRELA<sup>1</sup>, IRENEUSZ KORNECKI<sup>1</sup>

## Heat transfer and minimum wetting rate for a falling laminar liquid film

The problem of heat transfer and minimum wetting rate for the gravity-driven flow of a liquid film down a vertical tube is investigated. The paper provides also a description of the experimental setup and discussion of the obtained results compared with the results of a theoretical model of heat transfer assuming the laminar character of the liquid film flow under consideration.

### Nomenclature

$A$	- heat transfer area,	$T_{f1}$	- liquid temperature at inlet,
$C_p$	- specific heat at constant pressure,	$T_{f2}$	- liquid temperature at exit,
$d$	- pipe external diameter,	$U$	- voltage,
$h$	- heat transfer coefficient,	$\delta$	- film thickness,
$I$	- electric current,	$\epsilon_M$	- eddy diffusivity of momentum,
$L$	- test section length,	$\varphi$	- air relative humidity,
$\dot{m}$	- liquid mass flow rate,	$\lambda$	- thermal conductivity (also $k$ ),
$Nu$	- Nusselt number $Nu = h(\nu^2/g)^{1/3}/\lambda$ ,	$\mu$	- liquid dynamic viscosity,
$P$	- heater power, $P = UI$ ,	$\nu$	- liquid kinematic viscosity,
$Pr$	- Prandtl number, $Pr = \mu C_p/\lambda$ ,	$\rho$	- liquid density,
$Q_w$	- heat flux, $Q_w = UI$ ,	$\Gamma$	- unit mass flow rate, $\Gamma = \dot{m}/\Pi d$ ,
$q$	- heat flux density,	$\Delta T_1$	- wall-to-liquid temperature difference at inlet,
$r$	- pipe external radius,	$\Delta T_2$	- wall-to-liquid temperature difference at exit,
$Re$	- Reynolds number, $Re = 4\Gamma/\mu$ ,	$\Delta T_{log}$	- wall-to-liquid logarithmic temperature difference.
$T$	- temperature,		
$T_{w1}$	- wall temperature at inlet,		
$T_{w2}$	- wall temperature at half-length,		
$T_{w3}$	- wall temperature at exit,		

### Subscripts

$a$	- ambient,	$o$	- orifice, initial value,
$d$	- dry surface,	$r$	- rotameter,
$f$	- falling liquid,	$t$	- turbulent,
$g$	- heating,	$w$	- wall,
$i$	- film-gas interface,	-	- mean value.
$m$	- minimum value,		

<sup>1</sup>Institute of Fluid-Flow Machinery, Department of Thermodynamics and Heat Transfer, Fiszerka 14, 80-952 Gdańsk

## 1. Introduction

Heat transfer between the wall and falling liquid film has a great significance in chemical engineering as well as in other technical problems. Despite several years of investigations in this area, there are still questions not satisfactorily solved for practical applications. This is due to a complex character of the phenomenon which involves classical hydrodynamic problems connected with the character of motion (laminar or turbulent) and wave phenomenon on the film free surface. Additionally, a new phenomenon of instability of the liquid film flow comes into effect as for given conditions of liquid flow, including both the character of motion and surface type, there is a minimum film thickness below which the film loses its stability and splits into streams. This is an undesirable phenomenon because then the wall surface is only partially wetted which in turn deteriorates the conditions for heat transfer. The phenomenon was previously analysed in more detail by one author of the present paper [1]. The wave character of the liquid film motion can be observed for Reynolds numbers  $Re > 4$  [2]. Up to the some limiting value of Reynolds number, which after Brauer [3] can be estimated at approximately  $Re = 1600$ , the liquid film motion driven by gravity can be regarded as laminar because its mean geometrical thickness is, with good approximation, equal to the film thickness obtained from the Nusselt model elaborated to solve the momentum equation for a fully developed gravitational laminar film flow down a vertical wall. The Nusselt model gives the velocity distribution in the film and for a given flow rate enables the determination of its thickness vital for further determination of the heat transfer intensity. Usually, the problem is considered for two limiting conditions of a first and second kind, i.e.  $T_w = const$  and  $q_w = const$ . The second case embraces two possibilities with regard to the heat flux at the free surface  $q_i$ , assuming alternatively  $q_i = 0$  or  $q_i = q_w$ . A detailed derivation of a relation for the Nusselt number for both cases under consideration is given in Appendix. Nusselt's solutions concerning the heat transfer for the limiting condition  $T_w = const$  agree well with the experiments [4], whereas the results obtained in the papers [5-6], using the wall condition  $q_w = const$ , diverge significantly from the Nusselt model.

In the present work, investigations of heat transfer for a gravitational laminar liquid film flow using the condition  $q_w = const$  have been undertaken for a much wider range of Reynolds numbers. The aim of the investigations is to explain reasons for the above mentioned divergence. This is an important question, because in the range of laminar flow the model of Nusselt is used without any criticism what may lead to significant errors. The paper also provides a description of the experimental setup and comparison of obtained results with those of other investigators. Some preliminary results of liquid film breakdown into streams caused by the influence of heat flux are also presented – the situation when the increasing heat flux leads, through a so-called Marangoni effect, to the loss of liquid film stability.

## 2. Experimental setup

A schematic of the experimental setup and its description is presented in Fig. 1. The test rig was designed for measurements of heat transfer and liquid film breakdown concurrent and countercurrent with respect to the flowing air. At the first stage of experimental investigations, the measurements were conducted without the flow of air. In further experiments the authors intend to measure heat transfer conditions and film breakdown with the air flow.

The experimental setup consists of a few basic elements. These are: a header generating the liquid film 1, test section in the form of a copper vertical pipe of external diameter  $d = 0.034\text{m}$  and length  $L = 1.1\text{m}$ . Inside the pipe there is a heating element (heater) of length  $L_g = 1.07\text{m}$ . The measurements were conducted for the range of inlet water temperatures from 15 to 20°C and unit flow rate  $\Gamma = 0.016 \div 0.52\text{kg/ms}$  at the maximum heater power of 1200 W. The Reynolds number for a flowing film varied from 30 to 2000, therefore it can be assumed that the flowing film had a laminar character with the exception of some cases of higher Reynolds numbers investigated so as to test the dependence of the Nusselt number on the Reynolds number for  $Re > 1000$ . Thermal measurements of the rig were conducted in order to determine the heat transfer coefficient  $h$  whose values ranged from 400 W/m<sup>2</sup>K for the lowest water flow rates to 3000 W/m<sup>2</sup>K for the highest.

The heater was supplied from an autotransformer. Its power was determined on the basis of measurements of voltage  $U$  and current  $I$  flowing through it.

The most difficult part of the experimental work on hydrodynamics and heat transfer in connection with flowing liquid films is film generation. In experiments conducted by the authors of this paper the film was generated by an annulus slot distributor fixed to a supply header (see Fig. 1). Water was forced to a tank 16 and header 1 by a pump 7. Then in the form of a thin liquid film, it flowed down the pipe to the main tank 6, being simultaneously heated. From there it was pumped back to the circuit. It should be added that contrary to previous investigators [7], distilled water was used in present measurements, whose temperature was controlled to remain within the limits 15 ÷ 20°C.

Measured temperatures of the water and wall correspond to the points marked in Fig. 2. The wall temperature was measured by six thermocouples, two at each section – the beginning, middle and end of the investigated pipe.  $T_{f1}$  and  $T_{f2}$  are the temperatures of water at the inlet and exit, respectively, and  $T_a$  is the ambient temperature. At each pipe section, the wall temperatures were measured at two points symmetrically placed at the surface of the pipe in order to increase the accuracy of the measurements. The obtained results are gathered in Table 1, where subscripts such as '11' and '12' refer to the temperatures at section 1 in two symmetrical locations 1 and 2, and the temperature  $T_{w1}$  is determined by averaging of  $T_{w11}$  and  $T_{w12}$ , i.e.  $T_{w1} = (T_{w11} + T_{w12})/2$ .

Water flow rate measurements were performed using two rotameters 11 operating in the range of 5 ÷ 100kg/h and 100 ÷ 200kg/h, respectively, which for the

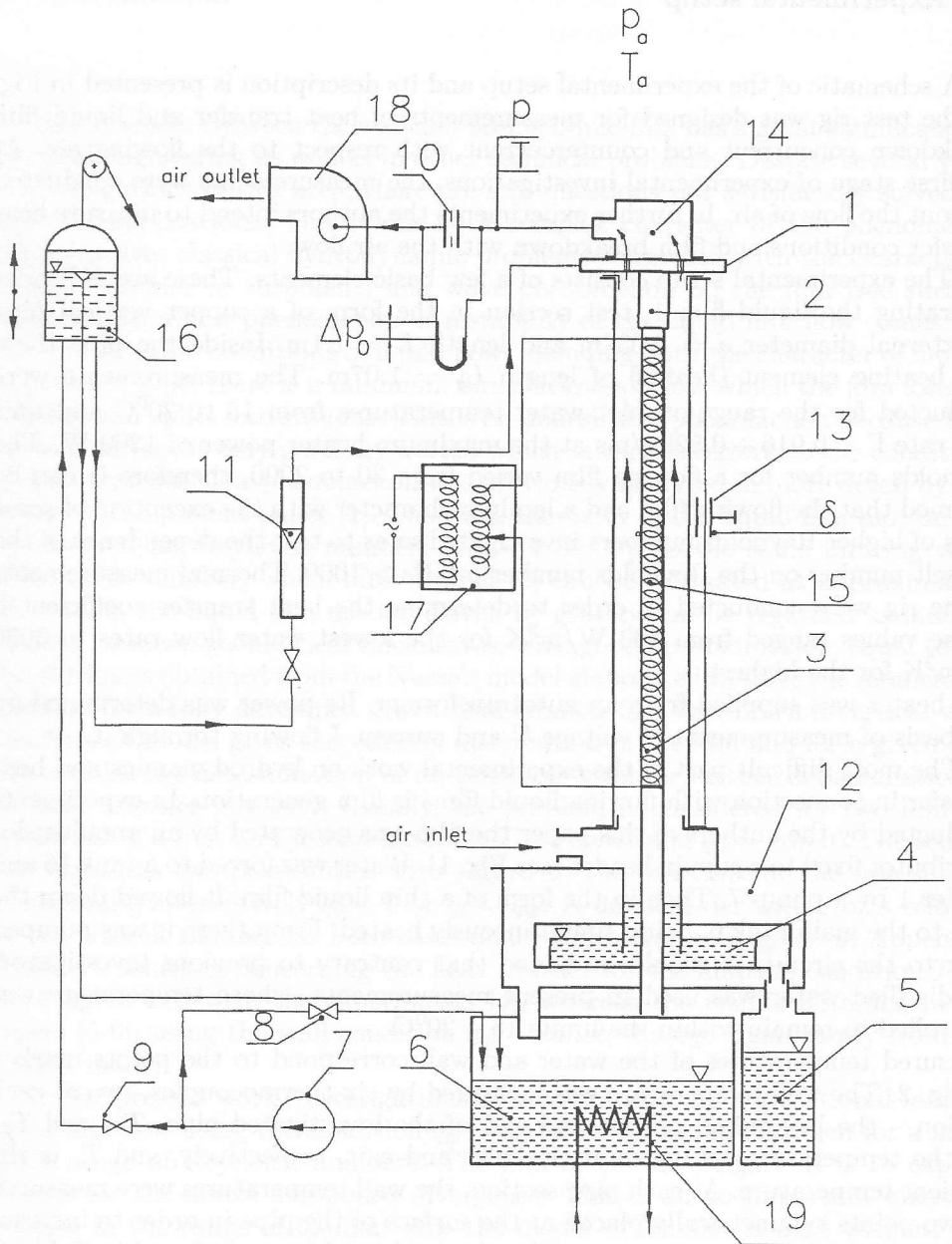


Fig. 1. A schematic of the experimental rig for investigations of the minimum wetting rate and heat transfer in thin liquid films: 1 - upper header, 2 - liquid film distributor, 3 - test section, 4 - water lock tank, 5 - measurement tank, 6 - main tank, 7 - water pump, 8 - overflow valve, 9 - cut-off valve, 10 - orifice, 11 - rotameter, 12 - lower tank, 13 - film thickness probe, 14 - air outlet pipe, 15 - electric heater, 16 - mobile tank, 17 - autotransformer, 18 - air fan, 19 - cooler.

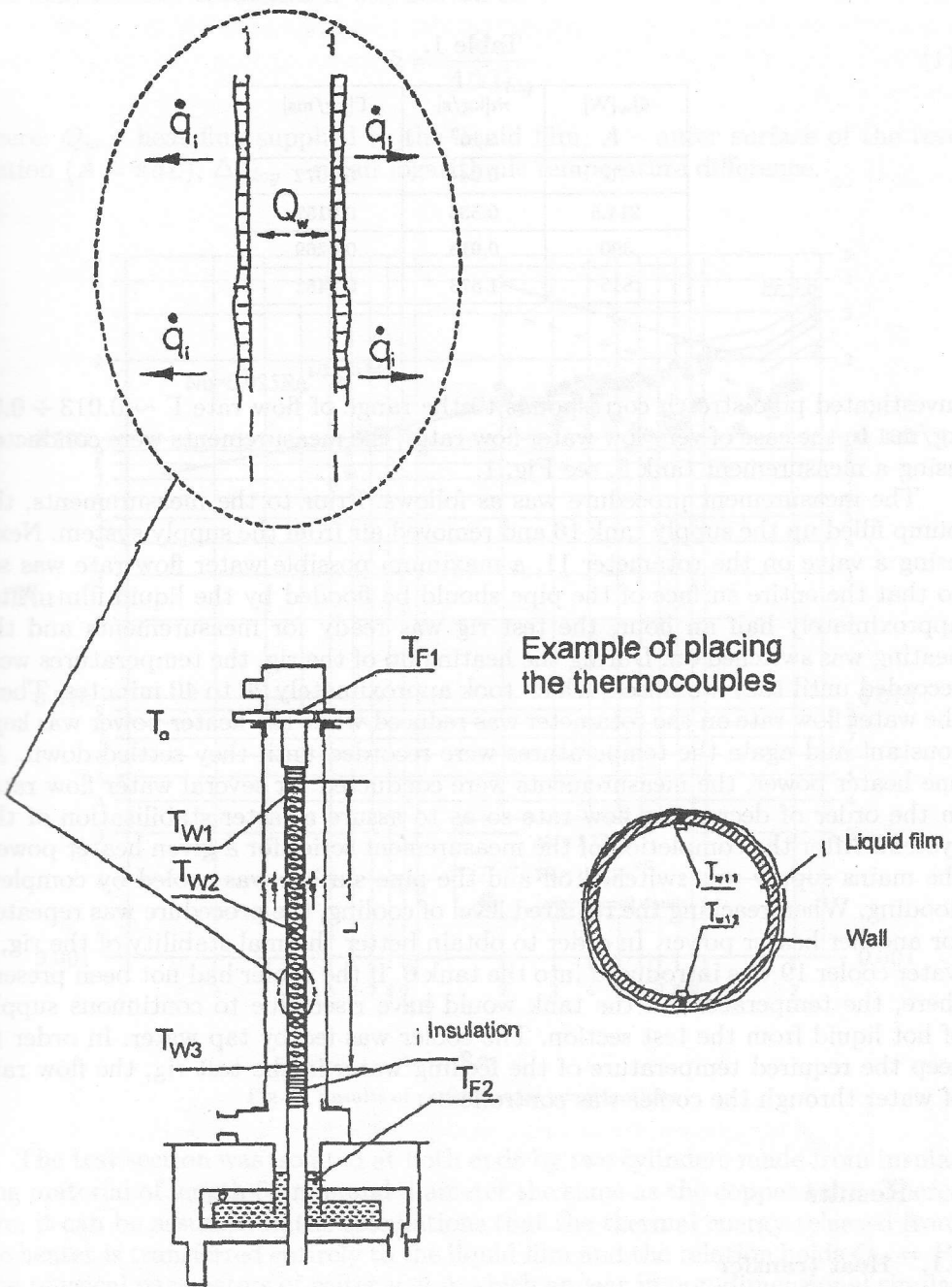


Fig. 2. A schematic distribution of temperature measurement points in the experimental rig as in Fig. 1.

Table 1.

$Q_w$ [W]	$\dot{m}$ [kg/s] $\times 10^3$	$\Gamma$ [kg/ms]
70	0.244	0.0072
214.5	0.536	0.0157
390	0.918	0.0269
815	1.573	0.0462

investigated pipe stretch corresponds to the range of flow rate  $\Gamma \sim 0.013 \div 0.52$  kg/ms. In the case of very low water flow rates, the measurements were conducted using a measurement tank 5, see Fig. 1.

The measurement procedure was as follows. Prior to the measurements, the pump filled up the supply tank 16 and removed air from the supply system. Next, using a valve on the rotameter 11, a maximum possible water flow rate was set so that the entire surface of the pipe should be flooded by the liquid film. After approximately half an hour, the test rig was ready for measurements and the heating was switched on. During the heating up of the rig, the temperatures were recorded until they stabilised, which took approximately 20 to 40 minutes. Then, the water flow rate on the rotameter was reduced while the heater power was kept constant and again the temperatures were recorded until they settled down. At one heater power, the measurements were conducted for several water flow rates in the order of decreasing flow rate so as to assure a faster stabilisation of the system. After the completion of the measurement series for a given heater power, the mains supply was switched off and the pipe surface was cooled by complete flooding. When reaching the required level of cooling, the procedure was repeated for another heater power. In order to obtain better thermal stability of the rig, a water cooler 19 was introduced into the tank 6. If the cooler had not been present there, the temperature in the tank would have risen due to continuous supply of hot liquid from the test section. The cooler was fed by tap water. In order to keep the required temperature of the feeding water in the test rig, the flow rate of water through the cooler was controlled.

### 3. Results

#### 3.1. Heat transfer

The experimental investigations were conducted according to the procedure described above for different values of wetting rate  $\Gamma$  and heater power  $P$ . The results of thermal measurements are presented in Appendix in Tables 1 and 2.



The heat transfer coefficient  $h$  was defined as

$$h = \frac{Q_w}{A \Delta T_{\log}} \quad (1)$$

where:  $Q_w$  - heat flux supplied to the liquid film,  $A$  - outer surface of the test section ( $A = \pi dL$ ),  $\Delta T_{\log}$  - mean logarithmic temperature difference.

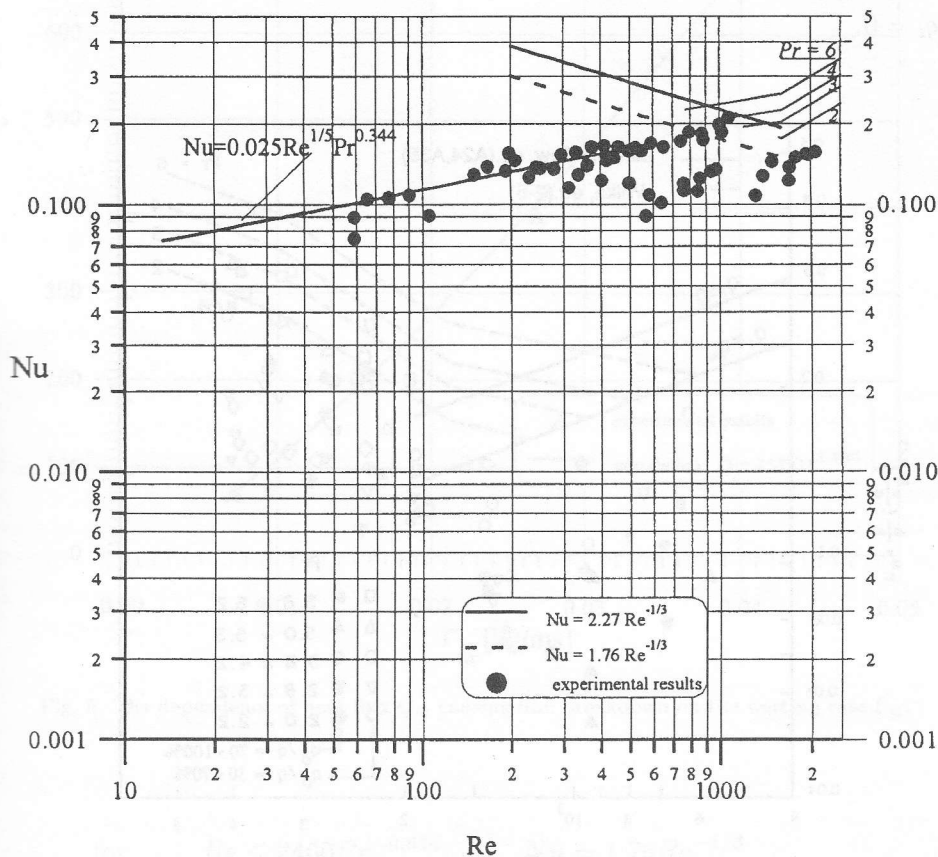


Fig. 3. Results of experimental investigations.

The test section was isolated at both ends by two cylinders made from insulating material of length 50 mm and diameter the same as the copper tube. Therefore, it can be assumed in the calculations that the thermal energy released from the heater is transferred entirely to the liquid film and the relation holds  $Q_w = P$ . The physical parameters of water  $\mu, \nu, \lambda$  which appear in non-dimensional similarity numbers  $Nu, Re, Pr$  have been calculated according to the mean temperature of water  $\bar{T}_f = (T_{f1} + T_{f2})/2$ .

The obtained results of investigations are presented in Fig. 3. Additionally,

for the sake of comparison, Fig. 3 exhibits the distribution of Nusselt number calculated by Wilke [4] using the Nusselt model, see Appendix, for the laminar and turbulent liquid film flow. Two characteristic equations result from the Nusselt model

$$Nu = 1,76Re^{-1/3} \tag{A24}$$

for  $q_i = q_w$  and

$$Nu = 2.27Re^{-1/3} \tag{A35}$$

for  $q_i = 0$ .

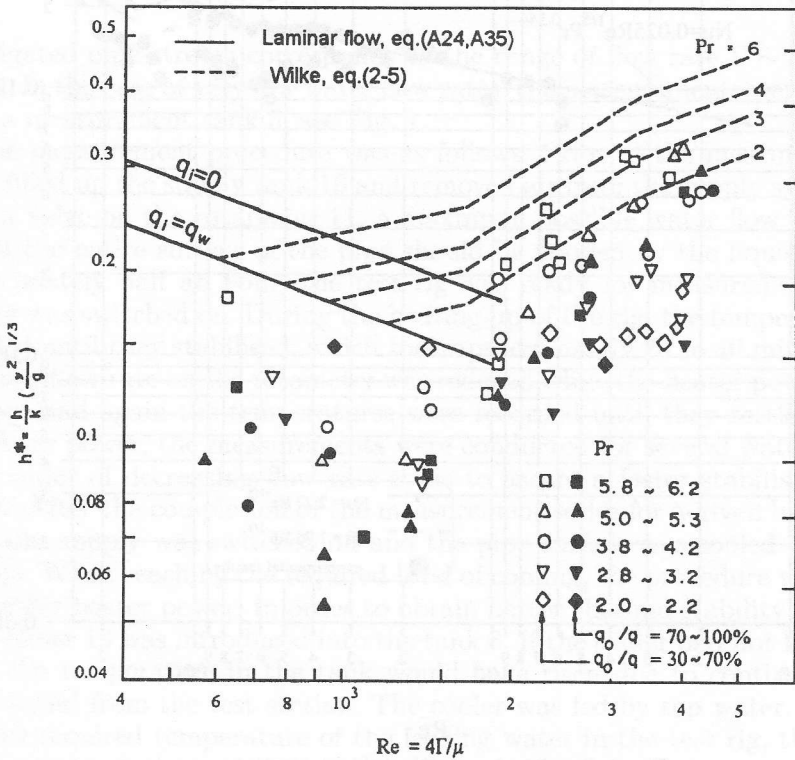


Fig. 4. Results of experimental investigations by Fujita and Ueda [5].

Also for the sake of comparison, the results of investigations by Fujita and Ueda [5] for the laminar and turbulent liquid film flow in a wide range of heat flux are presented in Fig. 4. The density of heat flux  $q_d$  corresponds to the situation where the film starts losing its stability and the formation of dry patches begins. Fig. 4 gives also display of experimental correlations worked out by Wilke [4] obtained based on investigations of Brauer [3] in a wide range of Reynolds number:

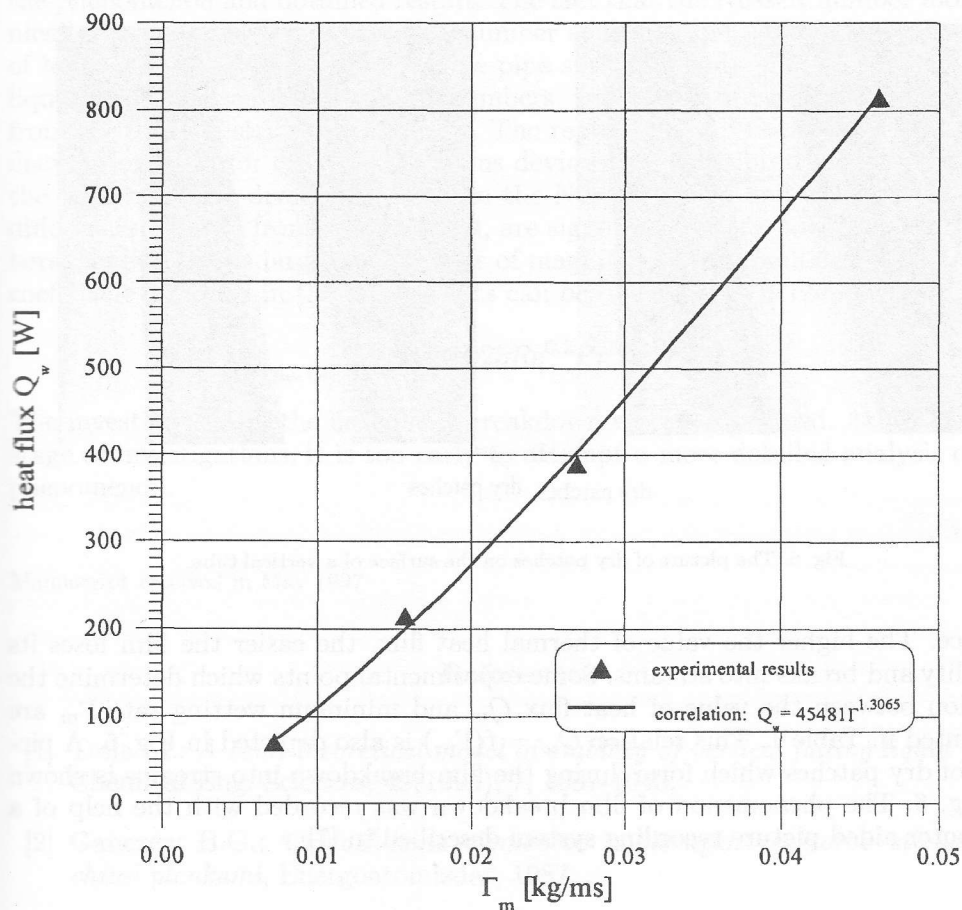


Fig. 5. The dependence of heat flux  $Q_w$  causing film breakdown on the wetting rate  $\Gamma_w$ .

$$\text{for } Re \leq 2460Pr^{-0.646}, \quad Nu = 1.76Re^{-1/3}, \quad (2)$$

$$\text{for } 2460Pr^{-0.646} \leq Re \leq 1600, \quad Nu = 0.0323Re^{1/5}Pr^{0.344} \quad (3)$$

$$\text{for } 1600 \leq Re < 3200 \quad Nu = 0.00102Re^{2/3}Pr^{0.344} \quad (4)$$

$$\text{for } 3200 \leq Re \quad Nu = 0.00871Re^{2/5}Pr^{0.344} \quad (5)$$

### 3.2. Film breakdown into streams

Besides the investigations of heat transfer, the phenomenon of film breakdown into streams due to the Marangoni effect [10-11] was also investigated. The film breakdown is connected with the gradient of surface tension on the waved film

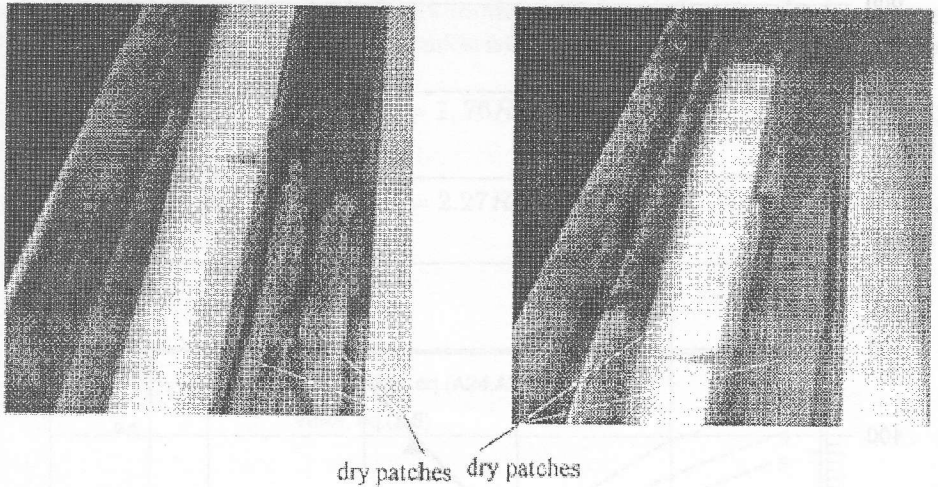


Fig. 6. The picture of dry patches on the surface of a vertical tube.

surface. The higher the value of thermal heat flux, the easier the film loses its stability and breaks into streams. Some experimental points which determine the relation between the value of heat flux  $Q_w$  and minimum wetting rate  $\Gamma_m$  are presented in Table 1. This relation  $Q_w = f(\Gamma_m)$  is also depicted in Fig. 5. A picture of dry patches which form during the film breakdown into streams is shown in Fig. 6. The phenomenon of film breakdown was recorded with the help of a computer aided picture recording system described in [7].

#### 4. Conclusions

The paper describes the results of investigations of heat transfer and film breakdown for a gravitationally falling liquid film down a vertical tube in a wide range of Reynolds number  $60 < Re < 2000$ . The obtained results are compared against the results of the Nusselt model for the laminar liquid flow. It has turned out that in the range of Reynolds numbers  $Re < 1000$ , the obtained results differ significantly from the theoretical values. The theory of liquid film hydrodynamics says that with the increasing Reynolds number, the Nusselt numbers decreases and the film thickness tends to increase. However, the investigations show that the increasing Reynolds number gives an opposite effect, i.e. leads to an increase of heat transfer intensity in the same way as in the case of turbulent motion. The obtained experimental results are consistent with the earlier results of Fujita and Ueda [5], see Fig. 4, in the same range of Reynolds numbers. At this stage it seems difficult to determine clearly the reason for the divergence between the theory of

the phenomenon and obtained results. The fact that the Nusselt number monotonically increases with the Reynolds number suggests that turbulent mechanisms of heat transfer come into play or the pipe surface is only partly flooded by the liquid film. At such low Reynolds numbers, the source of turbulence may come from the liquid distributor or header. The replacement of the applied slot liquid distributor with, for example, a porous device could possibly cast more light on the reason for the divergence between the Nusselt model and experiments. The differences, as seen from Figs. 3 and 4, are significant and for low Reynolds numbers can even be as large as one order of magnitude. The results of heat transfer coefficient obtained in the experiments can be described by a correlation:

$$Nu = 0.025 Re^{0.2} Pr^{0.344}. \quad (6)$$

The investigations of the liquid film breakdown will be continued. At the present stage of investigations, it is too early to attempt a more detailed analysis of the phenomenon.

Manuscript received in May 1997

### References

- [1] Trela M.: *A semi-theoretical model of stability of vertical falling liquid films*, Chemical Eng. Sciences, 49(1994), 7, 1007-1043.
- [2] Ganczew B.G.: *Okhlazhdenie elementov yadiernykh reaktorov stiekayushchimi plenkami*, Energoatomizdat, 1987.
- [3] Brauer H.: *Strömung und Wärmeübergang bei Rieselfilmen*, VDI-Forsch-Helf, 457, B22, 1956.
- [4] Wilke W.: *Wärmeübergang an Rieselfilmen*, VDI-Forsch-Helf, 490, B28, 1962.
- [5] Fujita T., Ueda T.: *Heat transfer to falling liquid films and film breakdown - I*, Int. J. Heat Mass Transfer, 21(1978), 2, 97-108.
- [6] Ganic E.M., Roppo N.M.: *A note on heat transfer to falling liquid films on vertical tubes*, Letters in Heat and Mass Transfer, 7(1980), 2, 145-154.
- [7] Trela M., Kornecki I., Ihnatowicz E.: *Investigations of minimum wetting rate and heat transfer of liquid film on a vertical surface - part I*, IFFM PAS internal report, 537/96, in Polish.
- [8] Ueda T., Tanaka T.: *Studies of liquid film flow in two-phase annular and annular-mist flow regions*, Bulletin of JSME, 17(1974), 107, 603-613.

- [9] Hewitt G.F., Hall Taylor H.S.: *Annular two-phase flow*, Pergamon Press, New York, 1970.
- [10] Zuber M., Staub F.W.: *Stability of dry patches forming in liquid films over heated surfaces*, Int. J. Heat Mass Transfer, 9(1966), 897-905.
- [11] Budiman, C.F. Florijanto, Palen J.W.: *Breakdown and evaporating falling films as a function of surface tension gradient*, Heat Transfer Engineering, 17(1996), 4, 72-81.

## Badania wymiany ciepła i minimalnego natężenia zraszania dla grawitacyjnego spływu filmu cieczowego

### Streszczenie

W pracy przedstawiono rezultaty eksperymentalnych badań wymiany ciepła i rozpadu filmu na strugi dla grawitacyjnego spływu warstewki cieczy w obszarze laminarnego charakteru ruchu. Opisano stanowisko eksperymentalne oraz sposób przeprowadzania badań. Uzyskane wyniki pokazały duże rozbieżności między modelem teoretycznym zjawiska (model Nusselta) a rezultatami badań. Te ostatnie są znacznie niższe od wartości teoretycznych. Podobne rezultaty badań są cytowane także przez innych autorów. Przyczyna tych rozbieżności nie jest znana. Wydaje to się być związane z typem urządzenia zraszającego oraz wpływem ruchu falowego. Podano także wstępne rezultaty badań rozpadu filmu spowodowane wpływem strumienia ciepłego.

## Appendix

Usually, the Nusselt model of laminar flow is used to describe the heat transfer for a liquid film freely falling down a vertical wall. However, by the Nusselt model we also understand the problem of heat transfer during condensation on a vertical wall. As these two Nusselt models differ from each other significantly, therefore in the text below, some fundamental relations for the lesser known Nusselt model of heat transfer in connection with a freely falling liquid film will be derived in brief. The process of derivation will also disclose the assumptions incorporated in the analysis. These considerations can be extended onto the case of film motion under shear stress or turbulent flow [8].

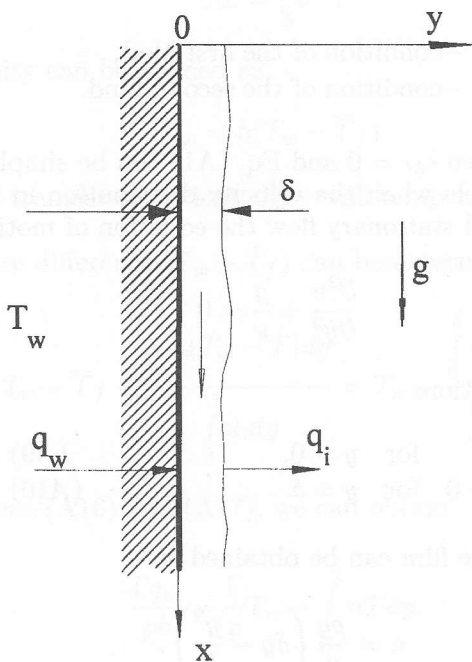


Fig. A1. The physical model of the phenomenon.

Neglecting the heat conductivity in the direction  $x$ , the energy equation for the stationary motion of a liquid film of thickness  $\delta$  and constant physical properties has a general form

$$u \frac{\partial T}{\partial x} = \frac{\partial}{\partial y} \left[ \left( \frac{\nu}{Pr} + \frac{\epsilon_M}{Pr_t} \right) \frac{\partial T}{\partial y} \right]. \quad (A1)$$

The boundary conditions are considered here for two characteristic cases with respect to the conditions at the free surface [8-9].

**No accumulation of heat in the film,  $q_i = q_w$**  In this case the boundary conditions can be presented as

$$x = 0 \quad T = T_i, \quad (A2)$$

$$y = \delta \quad T = T_i, \quad (A3)$$

$$y = 0 \quad \begin{cases} T = T_w & \text{—condition of the first kind,} \\ -\lambda \frac{\partial T}{\partial y} = q_w & \text{—condition of the second kind.} \end{cases} \quad (A4a, b)$$

**Thermal energy totally accumulated in the film,  $q_i = 0$ .** In this case the boundary conditions are as follows

$$x = 0 \quad T = T_0, \quad (A5)$$

$$y = \delta \quad T = T_0, \quad (A6)$$

$$y = 0 \quad \begin{cases} T = T_w & \text{—condition of the first kind,} \\ -\lambda \frac{\partial T}{\partial y} = q_w & \text{—condition of the second kind.} \end{cases} \quad (A7a, b)$$

If the flow is laminar, then  $\epsilon_M = 0$  and Eq. (A1) can be simplified. The solution of this equation is possible when the velocity distribution in the film is known. For a fully developed and stationary flow the equation of motion has a form

$$\frac{\partial^2 u}{\partial y^2} + \frac{g}{\nu} = 0 \quad (A8)$$

with the boundary conditions

$$u = 0 \quad \text{for } y = 0, \quad (A9)$$

$$\mu \frac{du}{dy} = 0 \quad \text{for } y = \delta. \quad (A10)$$

The velocity profile in the film can be obtained as

$$u = \frac{\rho g}{\mu} \left( \delta y - \frac{y^2}{2} \right). \quad (A11)$$

Below are derived relations for the Nusselt number for both cases mentioned above.

**No accumulation of heat in the film,  $q_i = q_w$ .** If the Reynolds number is defined as  $Re = 4\Gamma/\mu$ , then knowing that  $\Gamma = \rho\delta\bar{u}$  and incorporating the velocity profile as in Eq. (A11), we can obtain the following relation for the Reynolds number

$$Re = \frac{4\rho\delta}{\mu} \left\{ \frac{1}{\delta} \int_0^\delta u \, dy \right\} = \frac{4\rho}{\mu} \int_0^\delta \left[ \frac{\rho g}{\mu} \left( \delta y - \frac{1}{2} y^2 \right) \right] dy. \quad (A12)$$



Finally after integration we can get

$$Re = \frac{4\rho g}{3\nu\mu}\delta^3. \quad (A13)$$

Introducing a non-dimensional variable

$$\delta^* = \delta \left( \frac{g}{\nu^2} \right)^{1/3}, \quad (A14)$$

the expression (A13) for the Reynolds number takes the form

$$Re = \frac{4}{3}\delta^{*3}. \quad (A15)$$

The heat flux density can be defined as

$$q_w = h(T_w - \bar{T}_f) \quad (A16)$$

where  $h$  is the heat transfer coefficient,  $T_w$  - wall temperature and  $\bar{T}_f$  is the mean liquid temperature.

The temperature difference ( $T_w - \bar{T}_f$ ) can be determined from the relation

$$T_w - \bar{T}_f = \frac{\int_0^\delta u(T_w - T)dy}{\int_0^\delta u dy} = T_w - \frac{\int_0^\delta uTdy}{\Gamma/\rho}. \quad (A17)$$

From the expressions (A16) and (A17), we can obtain

$$\frac{\Gamma q_w}{\rho h} = \frac{\Gamma}{\rho} T_w - \int_0^\delta uTdy. \quad (A18)$$

In the considered case the heat flux in the film is constant along the co-ordinate  $y$ . Therefore, the temperature varies in a linear manner

$$T = T_w - \frac{q_w}{\lambda}y. \quad (A19)$$

Hence, the integral from Eq. (A18), bearing in mind the relations (A11), (A12) and (A19), is in the form

$$\int_0^\delta uTdy = T_w \int_0^\delta u dy - \frac{q_w}{\lambda} \int_0^\delta uydy = \frac{1}{4}\nu T_w Re - \frac{q_w}{\lambda} \int_0^\delta uydy. \quad (A20)$$

Taking into account Eq. (A11), we can obtain

$$\int_0^{\delta} u y dy = \int_0^{\delta} \frac{\rho g}{\mu} \left( \delta y^2 - \frac{1}{2} y^3 \right) dy. \quad (A21a)$$

which after integration gives

$$\int_0^{\delta} u y dy = \frac{5}{24} \frac{g}{\nu} \delta^4. \quad (A21b)$$

Placing Eqs. (A20) and (A21b) into (A18) gives:

$$\frac{\Gamma q_w}{\rho h} = \frac{\Gamma}{\rho} T_w - \frac{1}{4} \nu T_w Re + \frac{q_w}{\lambda} \int_0^{\delta} u y dy = \frac{q_w}{\lambda} \int_0^{\delta} u y dy. \quad (A22a)$$

And finally

$$\frac{\Gamma q_w}{\rho h} = \frac{5}{24} \frac{q_w g}{\lambda \nu} \delta^4. \quad (A22b)$$

Taking into account the relations (A22b) and (A14), we can get

$$Nu = \frac{h}{\lambda} \left( \frac{\nu^2}{g} \right)^{1/3} = \frac{6 Re}{5 \delta^{*4}}. \quad (A23)$$

Utilising further the relation (A15), we finally obtain:

$$Nu = \frac{6}{5} \frac{Re}{Re^{4/3}} \left( \left( \frac{4}{3} \right)^{4/3} \right) = \frac{6}{5} \left( \frac{4}{3} \right)^{4/3} Re^{-1/3} = 1.76 Re^{-1/3}. \quad (A24)$$

**Total accumulation of thermal energy in the film,  $q_i = 0$ .** In the case of laminar flow, the energy equation (A1) simplifies to the form

$$u \left( \frac{\partial T}{\partial x} \right) = \frac{\lambda}{\rho C_p} \left( \frac{\partial^2 T}{\partial y^2} \right). \quad (A25)$$

In the case of  $q_i = 0$ , the supplied heat goes entirely into the film to increase its energy. Then

$$\frac{\partial T}{\partial x} = \frac{\partial T_f}{\partial x} = \frac{q_w}{\Gamma C_p}. \quad (A26)$$

Placing the above relation into Eq. (A25), we obtain

$$\frac{\partial^2 T}{\partial y^2} = \frac{q_w u \rho}{\lambda \Gamma}, \quad (A27)$$

$$\frac{\partial T}{\partial y} = \frac{q_w \rho}{\lambda \Gamma} \int_0^y u \, dy - \frac{q_w}{\lambda}, \quad (\text{A28})$$

$$T - T_w = \frac{\rho q_w}{\lambda \Gamma} \int_0^y \left( \int_0^y u \, dy \right) dy - \frac{q_w}{\lambda} y. \quad (\text{A29})$$

Substituting Eq. (A11) into (A29) and keeping in mind that

$$\int_0^\delta u \, dy = \frac{\Gamma}{\rho} = \frac{1}{4} \nu Re = \frac{\nu}{3} \delta^{*3}$$

we can obtain

$$T = \frac{4q_w}{\lambda \nu \left(\frac{4}{3} \delta^{*3}\right)} \int_0^y \left( \int_0^y u \, dy \right) dy - \frac{q_w}{\lambda} y + T_w. \quad (\text{A30})$$

The integral in Eq. (A30) can be further transformed

$$\int_0^y \left( \int_0^y u \, dy \right) dy = \int_0^y \left( \int_0^y \left( \frac{\rho g}{\mu} \left( \delta y - \frac{1}{2} y^2 \right) \right) dy \right) dy = \int_0^y \left( \frac{\rho g}{\mu} \left( \frac{1}{2} \delta y^2 - \frac{1}{6} y^3 \right) \right) dy, \quad (\text{A31a})$$

and we can finally write

$$\int_0^y \left( \int_0^y u \, dy \right) dy = \frac{\rho g}{\mu} \left( \frac{1}{6} \delta y^3 - \frac{1}{24} y^4 \right). \quad (\text{A31b})$$

From Eqs. (A30) and (A31b), a relation for the temperature variation can be derived

$$T = \frac{4q_w}{\lambda \nu Re} \left( \frac{\rho g}{\nu} \left( \frac{1}{6} \delta y^3 - \frac{1}{24} y^4 \right) \right) - \frac{q_w}{\lambda} y + T_w. \quad (\text{A32a})$$

Taking into account the relation (A14), the temperature distribution takes the form

$$T = \frac{q_w}{\lambda} \left( -\frac{1}{24} \frac{g \rho}{\nu \Gamma} y^4 + \frac{g \rho \delta^*}{6 \nu \Gamma} \left( \frac{\nu^2}{g} \right)^{1/3} y^3 - y \right) + T_w. \quad (\text{A32b})$$

Substituting the above relation into Eq. (A18), we can obtain:

$$\frac{\Gamma q_w}{\rho h} = -\frac{q_w}{\lambda} \left\{ \frac{1}{48} \frac{\rho g^2}{\nu^2 \Gamma} \frac{1}{7} \delta^7 - \frac{1}{8} \frac{\rho g^2 \delta^*}{\nu^2 \Gamma} \left( \frac{\nu^2}{g} \right)^{1/3} \frac{1}{6} \delta^6 + \right.$$

$$\left. + \frac{1}{6} \frac{\rho g^2 \delta^{*2}}{\nu^2 \Gamma} \left( \frac{\nu^2}{g} \right)^{2/3} \frac{1}{5} \delta^5 - \frac{g}{8\nu} \delta^4 + \frac{g\delta^*}{3\nu} \left( \frac{\nu^2}{g} \right)^{1/3} \delta^3 \right\}. \quad (A33)$$

Finally introducing the variable  $\delta^*$  as in Eq. (A14) and multiplying both sides of Eq. (A33) by  $\frac{4\Gamma}{\nu^2 \rho}$ , we can obtain

$$Nu = \frac{h}{\lambda} \left( \frac{\nu^2}{g} \right)^{1/3} = \frac{Re^2/4}{-\frac{1}{7.12} \delta^{*7} + \frac{1}{12} \delta^{*7} - \frac{2}{15} \delta^{*7} + Re[\frac{1}{8} \delta^{*4} - \frac{1}{3} \delta^{*4}]}. \quad (A34)$$

Knowing that  $Re = \frac{4}{3} \delta^{*3}$  and hence  $\delta^* = (\frac{3}{4})^{1/3} Re^{1/3}$ , we finally arrive at a formula

$$Nu = \frac{Re^{-1/3}}{-\frac{26}{105} (\frac{3}{4})^{7/3} + \frac{5}{6} \frac{3}{3} (\frac{3}{4})^{7/3}} = 2.27 Re^{-1/3}. \quad (A35)$$

Table A1. Results.

No.	$\bar{m}$	$P[W]$	$T_{w11}$	$T_{w12}$	$T_{w21}$	$T_{w22}$	$T_{w31}$	$T_{w32}$	$T_{f2}$	$T_{f1}$	$T_a$	$\phi[\%]$
1	0.00059	0.0036	18.18	18.08	17.48	17.43	16.93	16.91	18.3	16.65	16	70
2	0.00059	0.0148	18.42	18.32	17.73	17.71	17.27	17.21	18.49	16.89	16	70
3	0.00058	0.1	18.95	18.79	18.81	18.8	18.6	18.51	18.98	18.98	16	70
4	0.001	0.14	22.32	22.22	21.72	21.71	21	21	22.3	20.72	16	70
5	0.00125	0.8	21.25	21.18	21.88	21.87	22.1	22.06	20.8	21.65	16	70
6	10	36	18.12	18.02	22	22.13	24.68	24.79	23.94	18.03	16	70
7a	5	107	18.76	18.61	31.1	31.33	34.32	34.6	33.38	15.7	14.0	58
7b	10	107	17.15	17.05	22.73	22.98	26.74	26.91	25.91	16.21	14.0	58
8a	5	182	20.97	20.79	41.53	41.96	44.69	45.1	43.99	15.85	12.0	62.5
8b	10	182	18.12	18.1	27.81	28.24	34.58	34.85	34	16.74	12.0	62.5
8c	20	182	17.62	17.55	21.92	22.4	25.55	25.73	24.72	16.72	12.0	62.5
8d	30	182	16.79	16.77	19.68	20.17	22.2	22.34	21.29	15.86	12.0	62.5
8e	40	182	17.08	17.1	19.27	19.76	21.03	21.28	20.15	16.0	12.0	62.5
8f	50	182	17.84	17.84	19.72	20.22	20.98	21.27	20.11	16.9	12.0	62.5
8g	60	182	17.82	17.82	19.44	19.93	20.19	20.47	19.45	16.94	12.0	62.5
9a	58	225	20.22	20.12	22.06	22.68	23.47	23.84	21.6	18.97	15.0	67
9b	66	225	20.03	19.96	21.53	22.24	22.72	23.0	21.13	18.84	15.0	67
9c	78	225	20.32	20.32	21.67	22.39	22.56	22.96	21.34	19.18	15.0	67
9d	86	225	20.8	20.77	22	22.72	22.68	23.05	21.38	19.7	15.0	67
9e	96	225	20.49	20.55	21.66	22.46	22.05	22.5	21.09	19.54	15.0	67
10a	58	400	20.49	20.47	24.33	25.55	26.9	27.55	24.19	18.8	16.0	66
10b	76	400	20.91	20.92	23.84	25.11	25.56	26.25	23.28	19.28	16.0	66
10c	86	400	21.2	21.2	23.96	25.29	25.12	25.82	23.0	19.61	16.0	66
10d	97	400	21.49	21.48	24	25.45	24.63	25.35	22.82	19.92	14.0	60
10d	140	400	23.44	21.17	20.64	22.04	18.68	18.6	18.91	16.89	14.0	60
10e	180	400	22.91	20.6	19.97	21.11	19.01	18.97	18.97	17.34	14.0	60

Table A1. Results (continued)

No.	$\dot{m}$	$P[W]$	$T_{w11}$	$T_{w12}$	$T_{w21}$	$T_{w22}$	$T_{w31}$	$T_{w32}$	$T_{f2}$	$T_{f1}$	$T_a$	$\phi[\%]$
10f	200	400	23.91	21.67	21.06	22.12	20.39	20.49	20.56	19.21	14.0	60
11a	5	415	25.18	25.05	66.07	66.42	66.4	66.9	64.44	15.41	13.0	61
11b	10	415	18.63	18.54	40.57	41.65	52	52.42	51.11	15.3	13.0	61
11c	20	415	17.58	17.5	27.77	28.8	35.97	36.35	34.6	15.59	13.0	61
11d	30	415	17.67	17.39	24.55	25.64	30.31	30.71	28.43	15.86	13.0	61
11e	40	415	18.15	18.11	23.34	24.39	27.67	28.12	25.48	16.45	13.0	61
11f	50	415	17.95	17.96	22.35	23.36	25.83	26.35	23.62	16.66	13.0	61
11g	60	415	17.67	17.67	21.92	22.88	25.07	25.73	22.46	16.0	13.0	61
12a	10	663	20.64	20.6	60.8	61.98	68.1	68.75	66.94	16.01	12.5	62.5
12b	20	663	18.6	18.53	36.54	38.57	49.4	50.12	47.1	16.05	12.5	62.5
12c	30	663	18.71	18.64	30.5	32.48	39.9	40.68	36.9	16.46	12.5	62.5
12d	40	663	18.76	18.75	27.63	29.6	34.5	35.4	31.22	16.69	12.5	62.5
12e	50	663	18.77	18.76	25.94	27.92	31.2	32.17	27.95	16.85	12.5	62.5
12f	60	663	18.37	18.38	24.67	26.57	28.72	29.8	25.62	16.67	12.5	62.5
13a	10	885	19.51	19.38	72.37	72.34	86.53	88.09	84.45	14.2	13.0	59
13b	20	885	19.38	19.22	41.9	44.45	56.5	57.27	53.79	16.39	13.0	59
13c	20	885	16.62	16.55	39.35	42.04	53.99	54.81	51.37	13.77	13.0	59
13d	30	885	18.64	18.6	34.16	36.65	45.56	46.55	42.15	16.15	13.0	59
13e	40	885	18.44	18.43	30.15	32.51	38.31	39.43	34.87	16.04	13.0	59
13f	50	885	18.65	18.66	28.92	31.04	34.94	36.31	31.26	16.37	13.0	59
13g	60	885	18.97	18.97	29.0	31.0	33.34	34.92	29.13	16.83	13.0	59
14a	98	900	21.58	21.67	28.69	32.06	29.34	31.0	26.36	19.43	16.0	66
14b	58	900	22.2	22.3	31.45	34.52	35.92	37.27	32.57	19.88	16.0	66
14c	68	900	21.98	22.09	29.96	33.05	33.74	35.23	30.39	19.85	16.0	66
14d	134	900	34.3	28.52	26.26	28.81	21.91	21.94	24.39	19.46	16.0	66
14e	168	900	32.83	26.32	24.34	27.28	21.24	21.31	23.03	18.9	16.0	66
14f	200	900	30.22	23.8	21.98	24.83	19.64	19.8	20.97	17.53	16.0	66
14d	83	900	21.82	21.94	29.09	32.25	31.37	33.02	28.03	19.69	16.0	66
15a	20	1156	21.89	21.75	53.34	57.06	71.97	73.92	69.16	18.2	14.0	58
15b	30	1156	21.04	20.94	42.0	45.78	55.57	56.7	51.64	18.04	14.0	58
15c	40	1156	20.4	20.34	36.52	40.05	46.23	47.55	41.98	17.6	14.0	58
15d	50	1156	20.43	20.39	34.27	37.57	42.22	42.73	36.73	17.63	14.0	58
15e	60	1156	21.34	21.32	33.43	36.55	38.59	40.26	33.94	18.69	14.0	58
16a	98	1225	22.76	22.77	31.6	36.57	33.13	35.07	29.86	20.12	17.5	63
16b	68	1225	23.37	23.36	34.43	38.56	38.85	40.93	35	20.72	17.5	63
16c	76	1225	23.34	23.38	34.18	38.63	37.66	39.72	33.65	20.68	17.5	63
16d	89	1225	23.1	23.16	32.39	37.17	35.04	37.16	31.55	20.44	17.5	63
16e	140	1225	38.9	31.06	28.02	31.66	22.39	22.46	26.28	19.7	15.0	62
16f	170	1225	37.88	29.43	26.6	30.24	22.28	22.41	25.33	19.64	15.0	62
16g	200	1225	36.83	28.16	25.48	28.89	22.16	22.29	24.37	19.67	15.0	62

Table A2. Results based on data from Table 1

No.	$\dot{m}$ [kg/s]	$\Gamma$ [kg/ms]	$P$ [W]	$T_{w1}$	$T_{w2}$	$T_{w3}$	$T_{f1}$	$T_{f2}$	$\Delta T_1$	$\Delta T_2$	$\Delta T_{log}$	$\Delta T_f$	$h$ [W/m <sup>2</sup> K]	$Re$	$Nu$
1	0.00059	0.0055	0.0036	18.13	17.45	16.92	16.65	18.3	1.48	- 1.38	-	1.65	-	-	-
2	0.00059	0.0055	0.0148	18.37	17.72	17.24	16.89	18.49	1.48	- 1.25	-	1.6	-	-	-
3	0.00058	0.0054	0.1	18.87	18.81	18.56	18.98	18.98	- 0.11	- 0.425	-	0	-	-	-
4	0.001	0.00936	0.14	22.27	21.72	21	20.72	22.3	1.55	- 1.3	-	1.58	-	-	-
5	0.00125	0.0117	0.8	21.22	21.88	22.08	21.65	20.8	- 0.435	1.28	-	- 0.85	-	-	-
6	0.00164	0.01453	36	18.07	22.06	24.73	18.03	23.94	0.04	0.795	0.2526	5.91	1179	58.67	0.09023
7a	0.00034	0.00305	107	18.69	31.22	34.46	15.7	33.38	2.985	1.08	1.874	17.68	472.3	13.45	0.03379
7b	0.00164	0.01453	107	17.1	22.86	26.82	16.21	25.91	0.89	0.915	0.9024	9.7	980.6	58.78	0.07494
8a	0.00034	0.00305	182	20.88	41.75	44.89	15.85	43.99	5.03	0.905	2.405	28.14	625.9	15.16	0.04082
8b	0.00164	0.01453	182	18.11	28.02	34.72	16.74	34	1.37	0.715	1.007	17.26	1494	65.14	0.1053
8c	0.00423	0.03746	182	17.59	22.16	25.64	16.72	24.72	0.865	0.92	0.8922	8	1687	150.3	0.1298
8d	0.00682	0.0604	182	16.78	19.93	22.27	15.86	21.29	0.92	0.98	0.9497	5.43	1585	229.6	0.1274
8e	0.00941	0.08333	182	17.09	19.52	21.16	16	20.15	1.09	1.005	1.047	4.15	1438	312.7	0.1167
8f	0.01201	0.1063	182	17.84	19.97	21.13	16.9	20.11	0.94	1.015	0.977	3.21	1541	403.2	0.124
8g	0.0146	0.1292	182	17.82	19.69	20.33	16.94	19.45	0.88	0.88	0	2.51	0	486.3	0
9a	0.01611	0.1426	225	20.17	22.37	23.66	18.97	21.6	1.2	2.055	1.589	2.63	1171	565.9	0.09087
9b	0.01833	0.1622	225	20	21.88	22.86	18.84	21.13	1.155	1.73	1.423	2.29	1308	639.1	0.1021
9c	0.02167	0.1917	225	20.32	22.03	22.76	19.18	21.34	1.14	1.42	1.275	2.16	1460	760.6	0.1133
9d	0.02389	0.2114	225	20.79	22.36	22.87	19.7	21.38	1.085	1.485	1.275	1.68	1460	844.5	0.1127
9e	0.02667	0.236	225	20.52	22.06	22.27	19.54	21.09	0.98	1.185	1.079	1.55	1724	937.4	0.1337
10a	0.01611	0.1426	400	20.48	24.94	27.23	18.8	24.19	1.68	3.035	2.291	5.39	1444	583.1	0.1094
10b	0.02111	0.1868	400	20.91	24.48	25.91	19.28	23.28	1.635	2.625	2.091	4	1582	760.1	0.1204
10c	0.02389	0.2114	400	21.2	24.63	25.47	19.61	23	1.59	2.47	1.998	3.39	1656	860.6	0.1259
10d	0.02694	0.2384	400	21.48	24.73	24.99	19.92	22.82	1.565	2.17	1.851	2.9	1787	972.2	0.1358
10e	0.0389	0.364	400	18.64	21.34	22.31	16.89	18.91	1.75	3.395	2.482	2.02	1333	1313	0.1086
10f	0.05	0.468	400	18.99	20.54	21.76	17.34	18.97	1.65	2.785	2.168	1.63	1526	1691	0.1237
10g	0.055	0.515	400	20.44	21.59	22.79	19.21	20.56	1.23	2.23	1.681	1.35	1968	1961	0.154
11a	0.00034	0.00305	415	25.12	66.25	66.65	15.41	64.44	9.705	2.21	5.065	49.03	677.6	18.47	0.03811
11b	0.00164	0.01453	415	18.59	41.11	52.21	15.3	51.11	3.285	1.1	1.997	35.81	1719	77.08	0.1065
11c	0.00423	0.03746	415	17.54	28.29	36.16	15.59	34.6	1.95	1.56	1.748	19.01	1964	166.9	0.1391
11d	0.00682	0.0604	415	17.53	25.09	30.51	15.86	28.43	1.67	2.08	1.868	12.57	1838	251	0.1375
11e	0.00942	0.08333	415	18.13	23.87	27.9	16.45	25.48	1.68	2.415	2.025	9.03	1695	336.4	0.1298
11f	0.01201	0.1063	415	17.95	22.86	26.09	16.66	23.62	1.295	2.47	1.82	6.96	1886	420.3	0.1468

Table A2. Results based on data from Table 1 (continued)

No.	$\dot{m}$ [kg/s]	$\Gamma$ [kg/ms]	$P$ [W]	$T_{w1}$	$T_{w2}$	$T_{w3}$	$T_{f1}$	$T_{f2}$	$\Delta T_1$	$\Delta T_2$	$\Delta T_{log}$	$\Delta T_f$	$h$ [W/m <sup>2</sup> K]	$Re$	$Nu$
11g	0.0146	0.1292	415	17.67	22.4	25.4	16	22.46	1.67	2.94	2.245	6.46	1529	499.4	0.1212
12a	0.00164	0.01453	663	20.62	61.39	68.42	16.01	66.94	4.61	1.485	2.759	50.93	1988	90.33	0.1094
12b	0.00423	0.03746	663	18.57	37.56	49.76	16.05	47.1	2.515	2.66	2.587	31.05	2120	192.3	0.1347
12c	0.00682	0.0604	663	18.68	31.49	40.29	16.46	36.9	2.215	3.39	2.761	20.44	1986	279	0.1368
12d	0.00942	0.08333	663	18.76	28.62	34.95	16.69	31.22	2.065	3.73	2.816	14.53	1947	361.6	0.1408
12e	0.01201	0.1063	663	18.77	26.93	31.69	16.85	27.95	1.915	3.735	2.724	11.1	2013	444.3	0.1499
12f	0.0146	0.1292	663	18.38	25.62	29.26	16.67	25.62	1.705	3.64	2.551	8.95	2149	523.9	0.164
13a	0.00164	0.01453	885	19.45	72.36	87.31	14.2	84.45	5.245	2.86	3.933	70.25	1861	105.1	0.09145
13b	0.00423	0.03746	885	19.3	43.17	56.89	16.39	53.79	2.91	3.095	3.002	37.4	2439	206.4	0.1469
13c	0.00423	0.03746	885	16.59	40.7	54.4	13.77	51.37	2.815	3.03	2.921	37.6	2506	196.3	0.1567
13d	0.00682	0.0604	885	18.62	35.41	46.06	16.15	42.15	2.47	3.905	3.133	26	2336	294.6	0.1543
13e	0.00942	0.08333	885	18.44	31.33	38.87	16.04	34.87	2.395	4	3.129	18.83	2339	374.4	0.1646
13f	0.01201	0.1063	885	18.66	29.98	35.63	16.37	31.26	2.285	4.365	3.214	14.89	2278	459.6	0.1651
13g	0.0146	0.1292	885	18.97	30	34.13	16.83	29.13	2.14	5	3.37	12.3	2172	547.8	0.1599
14a	0.02722	0.2409	900	21.63	30.38	30.17	19.43	26.36	2.195	3.81	2.929	6.93	2542	1019	0.1875
14b	0.01611	0.1426	900	22.25	32.98	36.59	19.88	32.57	2.37	4.025	3.125	12.69	2382	652	0.1654
14c	0.01889	0.1672	900	22.04	31.5	34.48	19.85	30.39	2.185	4.095	3.041	10.54	2448	745.3	0.1733
14d	0.02306	0.204	900	21.88	30.67	32.2	19.69	28.03	2.19	4.165	3.072	8.34	2423	883.4	0.1755
14e	0.0372	0.348	900	21.93	27.54	31.41	19.46	24.39	2.465	7.02	4.352	4.93	1710	1392	0.1285
14f	0.0467	0.437	900	21.27	25.81	29.57	18.9	23.03	2.375	6.545	4.114	4.13	1809	1697	0.1385
14g	0.055	0.515	900	19.72	23.41	27.01	17.53	20.97	2.19	6.04	3.795	3.44	1961	1930	0.1554
15a	0.00423	0.03746	1156	21.82	55.2	72.94	18.2	69.16	3.62	3.785	3.702	50.96	2583	242.8	0.1379
15b	0.00682	0.0604	1156	20.99	43.89	56.14	18.04	51.64	2.95	4.495	3.668	33.6	2606	331.1	0.1576
15c	0.00942	0.08333	1156	20.37	38.28	46.89	17.6	41.98	2.77	4.91	3.738	24.38	2557	412.1	0.1671
15d	0.01201	0.1063	1156	20.41	35.92	42.47	17.63	36.73	2.78	5.745	4.085	19.1	2341	496.5	0.1598
15e	0.0146	0.1292	1156	21.33	34.99	39.42	18.69	33.94	2.64	5.485	3.891	15.25	2457	592.1	0.1703
16a	0.02722	0.2409	1225	22.77	34.09	34.1	20.12	29.86	2.645	4.242	3.381	9.74	2997	1071	0.2126
16b	0.01889	0.1672	1225	23.37	36.5	39.89	20.72	35	2.645	4.89	3.653	14.28	2773	792.8	0.1871
16c	0.02111	0.1868	1225	23.36	36.41	38.69	20.68	33.65	2.68	5.04	3.737	12.97	2711	872.6	0.1852
16d	0.02472	0.2188	1225	23.13	34.78	36.1	20.44	31.55	2.69	4.55	3.539	11.11	2863	995.3	0.1995
16e	0.0389	0.364	1225	22.43	29.84	34.98	19.7	26.28	2.725	8.7	5.147	6.58	1968	1491	0.1449
16f	0.047	0.442	1225	22.34	28.42	33.66	19.64	25.33	2.705	8.325	4.999	5.69	2027	1782	0.1507
16g	0.055	0.515	1225	22.23	27.19	32.49	19.67	24.37	2.555	8.125	4.815	4.7	2104	2067	0.1578